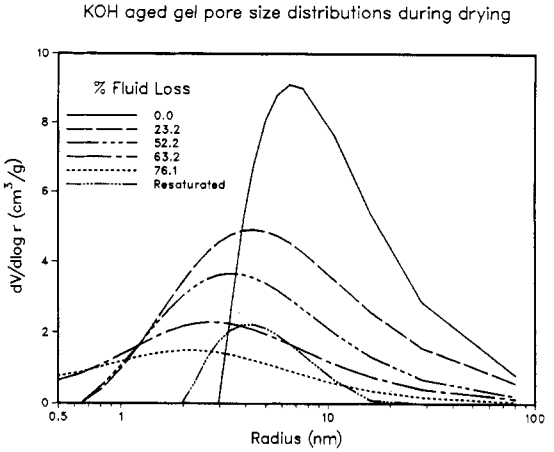

Figure 8. Pore size distributions at different solvent contents for the KOH-aged sample.

surface area change occurs and the pore radius, as determined via NMR, scales directly with pore volume. With respect to pore size, we note again that NMR results in the measurement of hydraulic radius (i.e., $r_p = 2V_p/A_s$). If the surface area is constant, the pore size should scale directly with pore volume, as is observed. The reason that the surface area undergoes no major change during the first 80% of drying is less clearcut. Apparently, the clusters forming the gel[23] undergo continued compaction during this first drying step without losing surface area. For example, this would result if additional branching during this step is minor, if there is relatively low coordination in the clusters and/or if the polymerization/depolymerization rate is low. In the final stages of drying, different mechanisms appear important for the KOH-aged and EtOH-aged samples. For the KOH-aged samples, the results may be interpreted as a stiff matrix that does not shrink under the influence of the capillary forces arising from the menisci penetrating the matrix. The pore volume becomes constant, but these large capillary forces result in the disappearance of surface roughness in the pores, resulting in a reduced surface area (and therefore, larger pore hydraulic radius). For the EtOH-aged sample, the matrix continues to shrink, resulting in very small final pore sizes (as observed with both NMR and N_2 desorption) and high surface area.

Acknowledgment. Support for this project has been provided by Sandia National Laboratories (Contract No. 02-2456 and 55-6778) under U.S. DOE Contract DE-04-76DP-00789. We thank S. Ross for the nitrogen adsorption measurements.

Nomenclature

A_s	specific surface area
$D(T_1)$	derivative of pore volume with respect to log (T_1)
$f(T_1)$	derivative of pore volume with respect to T_1
f_b	fraction of pore fluid with bulk fluid relaxation behavior
f_s	fraction of pore fluid with surface-affected relaxation behavior
L	sample length
L_0	initial sample length
L_f	sample length if completely dense
$\mathbf{M}(\tau)$	magnetization at time τ_1
$\mathbf{M}_0$	equilibrium magnetization
M_v	mass of solid sample/volume of fluid
r_p	hydraulic radius
T_1	spin–lattice relaxation time
$T_{1_{av}}$	average T_1
T_{1_b}	bulk fluid T_1
$T_{1_{min}}$	minimum expected T_1
$T_{1_{max}}$	maximum expected T_1
$T_{1_{surface}}$	T_1 of surface-affected phase
T_{1_s}	$T_{1_{surface}}/\Delta$
V	pore volume
V_0	pore volume before drying
V_p	specific pore volume
α	$1/T_{1_b}$
β	$2/T_{1_s}$
δ	optimum regularization smoothing parameter
Δ	thickness of surface-affected phase
τ	delay time between 180° and 90° pulses

Synthetic Study of Three Cesium Zirconates. Crystal Structure of Cs_2ZrO_3

Teng-Ming Chen and John D. Corbett*

Ames Laboratory—DOE[1] and Department of Chemistry, Iowa State University, Ames, Iowa 50011

Received June 9, 1988

The syntheses of cesium zirconates, potentially important sinks for fission-product cesium in Zircaloy-clad reactor systems, have been investigated for a diversity of reactions. The most effective synthetic routes involve reactions of elemental Cs and Zr with O_2 in open systems at slowly increasing temperatures or of finely divided ZrO_2 with Cs_2O (from Cs + CsO_2) in sealed silver tubing as the temperature is increased to 650–700 °C. Phase-pure Cs_2ZrO_3 has been obtained and shown to be isostructural with Cs_2PbO_3 (*Cmcm*, $Z = 4$, $a = 11.271$ (7) Å, $b = 7.743$ (4) Å, $c = 5.956$ (5) Å; R, $R_w = 5.1$, 5.8%). Two other cesium zirconates that contain a higher proportion of ZrO_2 have also been identified in mixtures produced by the second type of reaction. Their compositions have been estimated as $3Cs_2O{\cdot}7ZrO_2$ and $2Cs_2O{\cdot}7ZrO_2$ on the basis of the unit-cell volumes determined from single crystals of each together with known data for Cs_2ZrO_3 and the previously reported Cs_4ZrO_4.

Introduction

The identity and thermodynamic stability of any $mCs_2O{\cdot}nZrO_2$ phase are of prime importance with regard to the distribution of cesium, a major fission product, in Zircaloy-clad reactor fuel elements where there is an ample coating of ZrO_2 available on the cladding. The existence

0897-4756/89/2801-0040$01.50/0

of these zirconates is in turn especially significant relative to the potential, alternative combination of cesium with the less abundant fission-product iodine, particularly since iodine is clearly involved in stress-corrosion-cracking of the Zircaloys. A general consideration of the chemistry in the Cs–Zr–O–I system relevant to fission product behavior has recently appeared.[2] The only experimental evidence for a cesium zirconate in reactor systems has been a radioassay detection of the co-deposition of cesium and zirconium in the fuel-cladding gap in such a liquid water-cooled reactor element after an extensive burn-up.[3] On the other hand, the absence of any description of cesium zirconates in the chemical literature for many years has left their existence in doubt, in particular contrast to the well-documented existence of corresponding compounds with the other alkali metals such as K_2ZrO_3[4,5] and Rb_2ZrO_3.[6] Until very recently there was only the parenthetical remark in 1970 by Seeger and Hoppe[7] that a Cs_2ZrO_3 phase isostructural with the subject Rb_2PbO_3 had been identified by powder diffraction.

We undertook a synthetic investigation of the cesium zirconates because the absence of any information on these potentially important compounds intuitively seemed improbable in view of the high basicity and acidity expected for the respective components Cs_2O and ZrO_2. Actually, the absence of any report of the preparation of a cesium zirconate on a macroscopic scale probably has arisen mainly because of particular synthetic problems that originate with the limited stability of the precursor Cs_2O.[8] We have as a result of this study recently reported on the synthesis and structure of one product, Cs_4ZrO_4.[9] The present article describes the synthesis of the second, third, and fourth cesium zirconates we have been able to identify and, in some detail, the structure and properties of Cs_2ZrO_3, the most stable of all of these. In a recent article Cordfunke et al.[10] have also reported the synthesis of Cs_2ZrO_3 and its enthalpy of formation from calorimetric measurements.

Experimental Section

Materials. The sources and preparative methods employed for cesium (99.98%), α-CsO_2, high surface area ZrO_2, and powdered Zr (reactor grade) have been described before.[3,11] (We did not encounter any evidence for the reported β-CsO_2.[12]) All of these materials were handled only under dry conditions in a glovebox. The same precaution is necessary for the cesium zirconates as these are very susceptible to hydrolysis to CsOH and ZrO_2. Argon and oxygen of nominal 99.5% purity were dried by passage through freshly regenerated molecular sieves.

Containers. Most reactions were run in weld-sealed silver containers constructed from 9.4-mm-o.d. tubing, 0.64-mm wall (Engelhard Metals). These were loaded in the glovebox, crimped shut, and heliarc welded. This container was then sealed within a SiO_2 jacket under argon to protect it from attack by air in the resistance furnace. There was no evidence that the silver container participated in the reactions of interest. On the other hand, tantalum was observed to react with the cesium zirconates above ~680 °C to yield an unknown cesium tantalate and cesium metal. Zirconium containers caused decomposition above ~820 °C because of the formation of α-$Zr(O_x)$ solutions.

Syntheses. Classical reaction processes of the type in which finely divided ZrO_2 is allowed to react with incipient Cs_2O generated by the decomposition of compounds such as $CsNO_3$ or Cs_2CO_3 generally gave unsatisfactory results. No more than 5–10% conversion could be obtained regularly, and this product took the form of a thin, shiny coating on the ZrO_2 particles. The latter presumably arose because the limited diffusion of a cesium component into ZrO_2 at the temperatures of 600–1000 °C necessary for the decomposition of the oxo salts. A further problem with this reaction, particularly in open systems, doubtlessly arises from the limited stability of Cs_2O with respect to the elements,[8] which effectively limits the use of a Cs_2O reagent to either moderate temperatures or closed systems.

Cs_2ZrO_3. Samples of this compound that are single phase by Guinier powder patterns (and therefore conservatively estimated to be ≥95% in purity) can be consistently obtained in several ways. Perhaps the simplest is the slow reaction of flowing oxygen with a mixture of zirconium powder and a slight excess of cesium contained in a silver crucible. In this case, it is necessary to slowly preoxidize the cesium to CsO_2 starting at or near room temperature to avoid a destructive reaction that may even melt the silver crucible. Dilution of the oxygen with argon in the early stages is helpful. The reaction mixture is slowly heated to 650 °C over a period of up to a week. The reaction product may be ground and recharged with CsO_2, and the process repeated if necessary.

Excess CsO_2 in the product as well as the intermediates Cs_2O_2 and Cs_2O are easily decomposed and volatilized by heating in a vacuum above ~450 °C or under inert gas to about 700 °C.[8,13] A large excess of cesium in this reaction does not produce Cs_4ZrO_4, as the latter is decomposed to CsO_2 and Cs_2ZrO_3 by oxygen.[9] The use of zirconium metal strips instead of powder in this process has been observed to provide a lower yield of good crystals of Cs_2ZrO_3, probably because a slower reaction allows CsO_2 (melting point ~450 °C) (or CsO_x, $x < 2$) to function as a flux or solvent for Cs_2ZrO_3 (see below). Reactions of finely divided ZrO_2 with 100–200% excesses of CsO_2 in open silver crucibles under vacuum for 8 h at 435 °C also yield pure but poorly crystalline Cs_2ZrO_3 plus sublimed CsO_x.

As with the synthesis of Cs_4ZrO_4, reactions of stoichiometric proportions of Cs, CsO_2, and ZrO_2 within sealed silver tubing offer the best control of the reaction. Complete reaction of the ZrO_2 can be regularly obtained with care. A reaction process that proceeds from 400 to 650–700 °C over a period of 3–7 days is suitable, with the best results being obtained if an intermediate grinding of the product is included. The use of zirconium powder plus appropriately different proportions of Cs and CsO_2 at 700 °C for 7 days does not always work as well, and some ZrO_2 may remain in the product. The idea that CsO_2 dissolves Cs_2ZrO_3 is supported by the production of needle crystals of the latter when a 6:1 molar proportion of these reactants was heated for 34 days at 730 °C in sealed silver tubing. (Oxygen from CsO_x will of course slowly pass through the Ag wall into the SiO_2 jacket.) The decomposition of Cs_4ZrO_4 to Cs_2ZrO_3 plus Cs_2O occurs in a sealed tube near 730 °C,[9] but this temperature would be lowered appreciably through solution of the Cs_2O product in the excess CsO_2.

Poorly crystalline Cs_2ZrO_3 is also obtained from sealed-tube reactions of CsO_2 with excess Zr powder at 500–600 °C or, in low yield, from ZrO_2–Cs reactions as low as 360 °C, but both products are often contaminated with α-$Zr(O_x)$ as well as ZrO_2.

Phases 3 and 4. There are *at least* two additional cesium zirconates, both of which appear to contain a higher proportion of ZrO_2 than does Cs_2ZrO_3. We have not yet succeeded in producing a pure, macroscopic sample of either because of distinctly greater difficulties in achieving equilibrium than in the synthesis of Cs_2ZrO_3, yields so far being limited to ~40–50% of each. However, single crystals of both have been isolated, and, although their structures have not yet been solved, the apparent unit-cell

(1) The Ames Laboratory is operated for the U.S. Department of Energy by Iowa State University under Contract No. W-7405-Eng-82. This research was supported by the Office of Basic Energy Sciences, Materials Sciences Division.

(2) Chen, T.-M.; Kauzlarich, S. M.; Corbett, J. D. *J. Nucl. Mater.* **1988**, *151*, 237.
(3) Kleykamp, H. *J. Nucl. Mater.* **1979**, *84*, 109.
(4) Hagenmuller, P.; Tournoux, M. *Bull. Soc. Chim. Fr.* **1965**, 572.
(5) Gatehouse, B. M.; Lloyd, D. J. *J. Solid State Chem.* **1970**, *2*, 410.
(6) Hoppe, R.; Seeger, K. *Z. Anorg. Allg. Chem.* **1970**, *375*, 264.
(7) Seeger, K.; Hoppe, R. *Z. Anorg. Allg. Chem.* **1970**, *375*, 255.
(8) Klemm, E.; Scharf, H.-J. *Z. Anorg. Allg. Chem.* **1960**, *303*, 263.
(9) Chen, T.-M.; Corbett, J. D. *Z. Anorg. Allg. Chem.* **1987**, *553*, 50.
(10) Cordfunke, E. H. P.; Ouweltjes, W.; Van Vlaanderen, P. *J. Chem. Thermodyn.* **1987**, *19*, 1117.
(11) Smith, J. D.; Corbett, J. D. *J. Am. Chem. Soc.* **1985**, *107*, 5704.
(12) Dudarev, V. Y.; Tsentsiper, A. B.; Dobrolyubova, M. S.; *Sov. Phys.-Crystallogr. (Engl. Transl.)* **1974**, *18*, 477.
(13) Berardinelli, S. P.; Kraus, D. L. *Inorg. Chem.* **1974**, *13*, 189.

dimensions and space groups have been deduced therefrom. These data allow their respective 25–30-line powder patterns[2] to be completely indexed. Additionally, compositions have been estimated for each on the presumption that molar volumes deduced from the two known phases are transferable (see Results and Discussion section). Accordingly, the triclinic phase 3 is estimated to have a composition with Cs:Zr ~ 6:7 (i.e., $\sim 3Cs_2O{\cdot}7ZrO_2$) and the monoclinic phase 4, Cs:Zr ~ 4:7 ($\sim 2Cs_2O{\cdot}7ZrO_2$). These estimates are important relative to the synthetic conditions that maximize their yields, as follows.

Phase 4 is easier to produce than phase 3. A nonequilibrium mixture of this with Cs_2ZrO_3 and ZrO_2 is formed from reactions of Cs, CsO_2, and ZrO_2 with overall Cs:Zr proportions of ~4:7 in sealed silver tubing for 4–8 days at 650–700 °C. Phase 4 in a similar mixture has also been found as a product of reactions during which the silver container leaked and allowed Cs_2O to escape into the SiO_2 jacket, e.g., from those with starting proportions of 6:1, 1:1, and 4:7 under comparable reaction conditions. The effective compositions in the remaining samples were of course unknown. Phase 3 has also been observed in similar mixtures from comparable reactions with 6:1 and 1:1 initial compositions that leaked.

Phase 3, for which Cs:Zr is thought to be near 6:7, is obtained along with Cs_2ZrO_3 and ZrO_2 in a nonequilibrium mixture following similar Cs–CsO_2–ZrO_2 reactions near a Cs:Zr = 1:1 composition in a closed system for ~10 days at 670 °C. Alternatively, phase 3 is obtained either from the same three reactants or from CsO_2 + ZrO_2 mixtures with Cs:Zr between 3:2 and 2:3 when the materials were first preheated at 340–560 °C for 1–3 weeks and then allowed to react at 670–700 °C for 7–20 days. Products from this type of reaction with a Cs:Zr ratio of 1:1 do *not* contain Cs_2ZrO_3. Phase 4 is sometimes also found in these, especially with Cs:Zr ratios <1:1. However, *all* products of this two-stage type of reaction *also* exhibit a number of additional X-ray powder lines that must originate from yet another phase. The best single crystals of phases 3 and 4 were obtained from the latter, preheated type of reaction. Phase 3 as well as 4 also has been found mixed with ZrO_2 and, sometimes, Cs_2ZrO_3 after reactions in which the silver container leaked and therefore produced indefinite compositions (see above).

Analyses. The determination of the cesium and zirconium contents of a sample of Cs_2ZrO_3 that was single phase according to its Guinier pattern was carried out by atomic absorption, as before.[9] The observed (calculated) results were as follows: Cs, 64.68 (65.63); Zr, 23.30 (22.52) wt % (observed Cs/Zr = 2.000). Standard errors in each are estimated to be <3% and ~0.7%, respectively. Deviations of the individual data from theory are quite comparable to those similarly found for Cs_4ZrO_4,[9] while the single-crystal results for both indicate they possess substantially ideal stoichiometries.

X-ray Diffraction Studies. Preliminary product identification utilized X-ray powder diffraction film data collected with a focusing Guinier camera (Enraf-Nonius) equipped with a quartz monochromator to give clean Cu $K\alpha_1$ radiation. Sample mounting has been described previously.[14] Powdered silicon (NBS) was included as an internal standard, and the positions of the five observed lines of Si were fit to their known diffraction angles by a quadratic function. Lattice parameters for known structures were then determined by standard least-squares refinements of indexed data. Lattice constant and X-ray powder diffraction pattern data for the four cesium zirconates have already appeared.[2]

Blade-shaped single crystals of Cs_2ZrO_3 were mounted within thin-walled glass capillaries in a glovebox. Weissenberg photos established a C-centering condition. Two octants of data for the indicated orthorhombic cell were collected at room temperature on a DATEX diffractometer. The needle axis of the crystals was found to lie parallel to the crystallographic *c* (and chain) axis of the structure. Data collection and refinement parameters are summarized in Table I.

The C-centering condition, the additional extinction of *h*0*l*, *l* = 2*n* + 1 found in the reduced data, and the dimensions of the cell together with previous results on related compounds[15,16] all suggested that the phase's composition was Cs_2ZrO_3 and that the space group was $Cmc2_1$ or *Cmcm*. The successful refinement confirms the composition and the latter, centric space group, which serves to fix the O(2) atom on a 2-fold axis at $0,y,{}^1/_4$.

Table I. Crystallographic Data for Cs_2ZrO_3

space group	*Cmcm* (no. 63)
Z	4
cell param,[a] Å	
a	11.271 (7)
b	7.743 (4)
c	5.956 (5)
cryst size, mm	0.25 × 0.75 × 0.025
octants coll	*HKL*, $\bar{H}K\bar{L}$
$2\theta_{max}$, deg (Mo Kα)	50
no. of refl	
measd	965
obsd[b]	686
indep	219
absorp coeff, cm^{-1}	156.4
range of transm coeff	0.72–0.98
R_{av}, %	2.8
sec extinct coeff	0.16 (3) × 10^{-4}
R,[c] %	5.1
R_w,[d] %	5.8

[a] Typical Guinier powder data, Cu $K\alpha_1$ (λ = 1.54056 Å). [b] $I_o > 3\sigma(I_o)$; $F_o > 3\sigma(F_o)$. [c] $R = \sum||F_o| - |F_c||/\sum|F_o|$. [d] $R_w = [\sum w(|F_o| - |F_c|)^2/\sum w|F_o|^2]^{1/2}$, $w = 1/\sigma_F^2$.

The cesium atom was located from a three-dimensional Patterson projection, and the remainder of the atoms were found by successive Fourier syntheses. Convergence was obtained after refining positional and anisotropic parameters for all atoms, after which the R_w value was observed to decrease by 0.5% when a secondary extinction correction was included. Features in the final difference map were ≤0.5 e/Å^3; alternatively, simultaneous refinement of the occupancies of all but the cesium atom established that the compound was stoichiometric. The largest ratios found for B_{ii}/B_{jj} thermal parameters were 2.0 for heavy atoms and 2.7 for oxygen. Programs used for the absorption correction (ψ SCAN), refinement (ALLS), Fourier maps (FOUR), illustrations (ORTEP), etc., and the sources of the neutral-atom scattering factors (which included corrections for anomalous dispersion) have been cited before.[17]

Results and Discussion

Several cesium zirconates appear to be reasonably stable compounds, and their long absence from the literature seems to have been associated largely with synthetic problems deriving from the properties of the binary oxide reactants, namely, the low stability of Cs_2O with respect to the elements coupled with the refractory character of ZrO_2. The Cs_2O problem assessment is supported by the fact that M_2ZrO_3 as well as $M_2Zr_2O_5$ and other compositions have been obtained for M = Li–Rb rather readily. This circumstance applies for reactions of ZrO_2 with either the corresponding M_2O or a source of that compound such as M_2CO_3 or MNO_3.[4-6,18-20] In fact, comparable reactions involving the appropriate proportions of Cs_2O (from Cs plus CsO_2) and finely divided ZrO_2 give quantitative yields of Cs_2ZrO_3 as well as Cs_4ZrO_4 when carried out in sealed silver tubing at 650–700 °C, for example

$$3Cs + CsO_2 + 2ZrO_2 \rightarrow 2Cs_2ZrO_3$$

The Cs_2ZrO_3 phase can also be obtained in effect from CsO_2–ZrO_2 reactions in open silver crucibles under flowing

(14) Daake, R. L.; Corbett, J. D. *Inorg. Chem.* **1978**, *17*, 1192.
(15) Panek, P.; Hoppe, R. *Z. Anorg. Allg. Chem.* **1972**, *393*, 13.
(16) Hoppe, R.; Stöver, H.-D. *Z. Anorg. Allg. Chem.* **1977**, *437*, 123.
(17) Hwu, S.-J.; Corbett, J. D.; Poeppelmeier, K. R. *J. Solid State Chem.* **1985**, *57*, 43.
(18) Claverie, J.; Fouassier, C.; Hagenmuller, P. *Bull. Soc. Chim. Fr.* **1966**, 244.
(19) Dittrich, G.; Hoppe, R. *Z. Anorg. Allg. Chem.* **1969**, *371*, 306.
(20) Gatehouse, B. M.; Lloyd, D. J. *J. Solid State Chem.* **1970**, *1*, 478.

Table II. Atomic Positions and Equivalent Isotropic Thermal Parameters in Cs_2ZrO_3

atom	posn	x	y	z	B_{iso}, Å^2
Cs	8g	0.33643 (8)	0.1450 (1)	0.25	2.13 (5)
Zr	4c	0	0.0828 (2)	0.25	1.34 (8)
O(1) (base)	8e	0.1175 (8)	0	0	1.9 (4)
O(2) (apex)	4c	0	0.3295 (19)	0.25	2.5 (7)

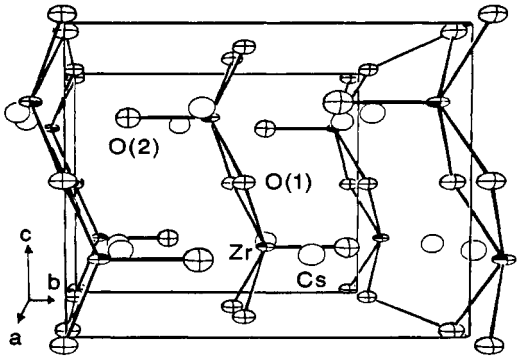

Figure 1. Structure of Cs_2ZrO_3 showing portions of the infinite $Zr(O)O_{4/2}$ chains that run parallel to $\vec{c}$. The view is down the long a axis. Uncrossed atoms are cesium (50% thermal probability ellipsoids).

oxygen (see Experimental Section). On the other hand, the isolation reported for Cs_2ZrO_3 following a water wash of the products of a $ZrSiO_4$–CsOH reaction[21] is highly improbable because of the high hydrolytic sensitivity of the zirconates.

Cordfunke et al.[10] have very recently also reported the synthesis of Cs_2ZrO_3 by reaction of CsO_2 with ZrO_2 at ~600 °C in silver containers equipped with screw caps, an intermediate regrinding of the product also being included. They also determined $\Delta H°_f$ for the phase calorimetrically. The weak violet color they report for this product is unusual, as all of our products have been white.

The phase Cs_2ZrO_3 appears to be the most stable ternary compound in the Cs–Zr–O system as far as thermal decomposition is concerned, yielding Cs_2O and ZrO_2 somewhat above 900 °C either in a sealed silver container or under high vacuum. The corresponding decomposition temperatures for Cs_4ZrO_4 are about 730 and 275 °C, respectively. Preliminary experiments with the two other phases, phases 3 and 4 (below), suggest that these have an intermediate stability with respect to disproportionation into Cs_2ZrO_3 and ZrO_2 under vacuum conditions.[2]

The crystal structure of Cs_2ZrO_3 is illustrated in Figure 1 by a view of the unit cell, while Tables II and III contain the structural parameters and important distances, respectively. The structure is the same as that recently described for Cs_2PbO_3.[22] The anion in Cs_2ZrO_3 exhibits an interesting infinite chain structure of square-pyramidal ZrO_5 units that face in alternate directions and share trans basal edges, viz., $^1_\infty[Zr(O)O_{4/2}^{2-}]$. Especially noteworthy is the short Zr–O(2) distance for the apically bonded oxygen, 1.90 Å, a value appropriate to the presence of multiple bonding. Similar but puckered chains are already known in K_2ZrO_3,[5] while this is the first zirconium example in which the shared basal oxygen atoms all lie in the (020) planes, which means that the axial Zr–O bonds along the chain lie parallel to $\vec{b}$ and alternate in direction. The puckering observed in K_2ZrO_3, etc., is achieved from this structure by rotating the $Zr(O)O_{4/2}$ units in alternate directions about axes through the metal and parallel to $\vec{a}$ (Figure 1). The basis for this distortion as a function of alkali-metal size and coordination has recently been considered for the series $(K,Rb,Cs)_2PbO_3$ by Stoll and Hoppe.[22] The oxygen polyhedron about cesium provides a low-symmetry five-plus-two coordination, one that is largely determined by the chain structure.

Table III. Relevant Bond Distances (angstroms) and Bond Angles (degrees)[a] in Cs_2ZrO_3

Intrachain Distances			
Zr–4[b] O(1)	2.091 (6)	O(1)–O(1)	2.65 (2)[c]
Zr–O(2)	1.91 (2)	O(1)–2 O(1)	2.969 (1)
Zr–2 Zr	3.233 (2)	O(2)–4 O(1)	3.23 (1)
Interchain Distances			
Zr–2 O(2)	4.35 (1)	Cs–2 O(1)	3.093 (7)
O(1)–2 O(1)	3.98 (2)	Cs–2 O(1)	3.161 (2)
O(2)–2 O(2)	3.97 (2)	Cs–O(2)	3.06 (1)
Cs–Cs	3.693 (2)	Cs–2 O(2)	3.502 (1)
Angles			
O(1)–Zr–O(2)	107.81 (7)		
O(1)–Zr–O(1)	78.7 (4), 90.5 (3)		
Zr–O(1)–Zr	101.3 (4)		

[a] Within the same chain. [b] Number of equivalent atoms. [c] Between bridging atoms.

Table IV. MAPLE Results for Cs_2ZrO_3 (kcal/mol)

	binary	ternary	Δ
Cs^+	2 × 103.7	2 × 106.9	+6.4
Zr^{4+}	1945.3[a]	1809.9	−135.4
$O(2)^{2-}$	324.4	468.0	+143.6
$O(1)^{2-}$	2 × 543.9[a]	2 × 539.5	−8.8
Σ	3564.9	3570.7	5.8 (=0.16%)

[a] Monoclinic ZrO_2, with the mean oxygen value.

The structures of the cesium and potassium phases are distinguished in detail by a choice of orthorhombic space groups. The K_2ZrO_3 with the puckered $Zr(O)O_{4/2}$ layers and, more recently, $(K,Rb)_2PbO_3$ have been established to occur in space group *Pmcn*. The correct space group for the phase with planar sheets of shared oxygen atoms is *Cmcm*, the acentric $Cmc2_1$ originally assigned to Cs_2PbO_3 having been corrected recently.[22] Likewise, Cs_2ZrO_3 was originally[6] and then again recently[10] assigned the K_2ZrO_3 structure on the basis of their Debye–Scherrer X-ray powder patterns. In practice, it may not be possible to distinguish the *Pmcn* symmetry from the correct assignment *Cmcm* in this way since the C-centering violations in the former case are likely to be weak. (For example, see the F_o/F_c data reported for Rb_2PbO_3.[7]) The Debye–Scherrer pattern of Rb_2ZrO_3[6] similarly fits the C-centering category, although the phase was assumed at the time to have the lower symmetry of the potassium analogue. The true symmetry of the rubidium compound appears to be problematical at this time.

Valuable insights into the solid-state conversions of binary into ternary (or higher) phases, such as that typified by the reaction

$$Cs_2O + ZrO_2 \rightarrow Cs_2ZrO_3$$

are provided by comparison of MAPLE[23] sums for the reactants relative to that of the product, that is, sums of partial Madelung energies for the individual ions. This empirical approach presumably works because changes in the overall bonding and in the energy are not large in

(21) Alyamovskaya, K. V.; Chukhlantsev, V. G. *Inorg. Mater. (Engl. Transl.)* **1979**, *15*, 1990.
(22) Stoll, H.; Hoppe, R. *Z. Anorg. Allg. Chem.* **1987**, *551*, 151.
(23) Madelung part of the lattice energy: Hoppe, R. In *Crystal Structure and Chemical Bonding in Inorganic Chemistry*; Rooymans, C. J. M., Rabenau, A., Eds.; North-Holland: Amsterdam, 1975; p 127; *Angew. Chem., Int. Ed. Engl.* **1970**, *9*, 25.

reactions that involve only solids. Oxides and fluorides have been tested particularly well.[23] This comparison also provides a valuable "check" on the correctness of a structure, especially one in which the light atoms such as oxygen may not have been located very well by X-rays but in which these atoms contribute significantly to the Madelung energy. The model implies *not* that simple ionic bonding pertains but only that the character of the bonding does not change significantly during the formation reaction.

MAPLE calculations for Cs_2ZrO_3 based on the data in Table II have kindly been provided by Professor Hoppe[24] and are listed in Table IV. The conversion of Cs_2O with its layered, anti-$CdCl_2$-type structure into the ternary phase obviously provides significantly improved bonding for the oxygen from the alkali-metal phase—basically the essence of an acid–base reaction—and this gain compensates for the loss calculated for zirconium that accompanies its conversion from seven to five coordination. A noteworthy and supportive result of these calculations and the structure is that the sum of the Madelung energies for Cs_2ZrO_3 agrees with that for the binary portions to within 5.8 kcal, which is only 0.16% of the large numbers that make up the difference. The corresponding difference for the published structure of Cs_4ZrO_4[9] is +42.3 kcal or 1.0% of that of the components.[24] It has been argued that the values used for Cs_2O are unrealistically low because of the layered nature of the phase and that a value of a hypothetical three-dimensional structure, analogous to those of other MOH and MF phases, should be used.[24] This in fact will decrease the result for Cs_4ZrO_4 to 33.2 kcal and that for Cs_2ZrO_3 (Table IV) to −3.3 kcal, but the difference between the two structures still remains.

The slowness with which cesium zirconates are formed and interconverted is emphasized by our synthetic studies. These have established both the ways in which Cs_4ZrO_4 and Cs_2ZrO_3 can be prepared in quantitative reactions and the existence of at least two more cesium zirconates that form only with greater difficulty. The latter occur (see Experimental Section for details) in systems containing more ZrO_2, and either their rates of formation are sufficiently low *or* the correct synthetic conditions have not yet been employed, that only a 40–50% yield of each together with other phases in a nonequilibrium mixture has been obtained. The so-called phase 4 appears to contain the highest proportion of ZrO_2, and this together with ZrO_2 and Cs_2ZrO_3 are found for Cs:Zr compositions near 4:7. Phase 3 forms less readily and occurs only at intermediate compositions near 1:1 *or* over a wider composition range when the intiial CsO_x–ZrO_2 mixtures are intially allowed to react at lower temperatures (340–560 °C) before being heated to 690–700 °C. Yet another phase appears to be present in the latter cases as well.

Fortunately, single crystals of both phases 3 and 4 have been isolated, and these have allowed the unit-cell parameters[25] and the probable space group of each to be determined ($P\bar{1}$ for phase 3, $P2_1/m$ for phase 4 for the centric choice for each). The credibility of these assignments is supported by the fact that these results allow complete indexing of their respective Guinier powder patterns. We note that Cs_4ZrO_4 as well as crystals with unit-cell dimensions and symmetries that we associated with phases 3 and 4 have also been observed by Hoppe and co-workers[24,26] but not by Cordfunke et al.[10]

Table V. Observed and Estimated Compositions and Cell Volumes (Å^3) for the Cesium Zirconates

Cs_2O:ZrO_2	phase or emp formula	space group	$Z\cdot(n)$	V_{obsd}	V_{calcd}
2:1	Cs_4ZrO_4	$P2_1/c$	4	940 (2)[a]	
1:1	Cs_2ZrO_3	$Cmcm$	4	520 (1)[b]	
	phase 3	$P\bar{1}$	2	996 (1)[c]	
3:7	$Cs_6Zr_7O_{17}$				980[d]
	phase 4	$P2_1/m$		3066 (2)[c]	
2:7	$Cs_4Zr_7O_{16}$		4 (2)		3080
(8:27	$Cs_{16}Zr_{27}O_{62}$		2		3030)
(1:2	$Cs_2Zr_2O_5$[e]		4 (5)		3100)
(1:6	$Cs_2Zr_6O_{13}$[e]		4 (3)		3060)

[a] Reference 9. [b] This work. [c] Reference 25. [d] Based on $V(Cs_2O)$ = 105 Å^3 and $V(ZrO_2)$ = 25 Å^3 derived from data for the first two phases. [e] Outside of apparent field of stability.

The unit-cell data for the four cesmium zirconates together with space-filling principles ("Raumchemie"[27]) allow the compositions of the third and fourth phases to be estimated, as shown in Table V. Cell volumes for the well-established compositions and structures of Cs_4ZrO_4 and Cs_2ZrO_3 provide partial volumes of 105 and 25 Å^3 per formula unit for Cs_2O and ZrO_2, respectively (Table V). (Data for the corresponding, isostructural lead compounds[22,28] yield 106 Å^3 for Cs_2O, while Biltz' ionic increments[27] give 105 and 40–41 Å^3 for Cs_2O and ZrO_2, respectively.) These data in turn yield an unambiguous prediction of Cs_2O:ZrO_2 = 3:7, $Cs_6Zr_7O_{17}$, for phase 3 and the probable (simplest) value of 2:7, $Cs_4Zr_7O_{16}$, for phase 4. The latter with its relatively large cell also allows for closely similar but more complex formulations such as 8:27 ($Cs_{16}Zr_{27}O_{62}$, Z = 2), but these do not represent significant improvements. Alternative solutions of the algebra that give Cs_2O:ZrO_2 = 1:2 ($Cs_2Zr_2O_5$) or 1:6 ($Cs_2Zr_6O_{13}$) for phase 4 seem to lie outside of the composition region suggested by conditions that favor its formation, and the first case denies the fact that phase 4 appears to lie on the ZrO_2 side of phase 3. All of these predictions are still somewhat tenuous, however, as they depend on the interpretation of the results of incomplete equilibrations and on the transferability of cell volumes for unknown structures.

The synthesis and characterization of the cesium zirconates are of particular importance with respect to the fission-product chemistry in liquid-water-cooled reactors since cesium is the predominant fission product and the Zircaloy cladding possesses an ample ZrO_2 coating. We were drawn to the question of the virtual nonexistence of cesium zirconates implied by the literature by the intuitive position that their instability was thermodynamically unreasonable. Their presence is especially important regarding precursors to stress–corrosion–cracking. Although the less abundant iodine seems to be clearly responsible for these failures, thermodynamic modeling of the situation in the absence of evidence for, or data on, any cesium zirconate has led to predictions that CsI would be the primary equilibrium state of fission-product iodine. In fact, the unlikelihood of this and the importance of Cs_2ZrO_3 (or one of the other zirconates) can both be demonstrated by recent observations that CsI reacts with excess ZrO_2 to form small amounts of Cs_2ZrO_3 on the ZrO_2 particles plus ZrI_4 (probably as Cs_2ZrI_6).[2] This reaction is limited on a synthetic scale by familiar kinetic factors associated with

(24) Hoppe, R., private communications, 1985–6.
(25) Phase 3 (~$3Cs_2O{\cdot}7ZrO_2$): a = 10.250 (1) Å, b = 10.416 (2) Å, c = 10.104 (1) Å, α = 106.45 (1)°, β = 98.51 (1)°, γ = 100.17 (1)°. Phase 4 (~$2Cs_2O{\cdot}7ZrO_2$): a = 9.926 (5) Å, b = 15.359 (8) Å, c = 10.642 (8) Å, β = 103.28 (3)°.[2]
(26) Kröschell, P.; Hoppe, R., private communication, 1985.
(27) Biltz, W. *Raumchemie der festen Stoffe*; Leopold Voss Verlag: Leipzig, Germany, 1934.
(28) Martens, K.-P.; Hoppe, R. *Z. Anorg. Allg. Chem.* **1980**, *471*, 64.

the effective conversion by ZrO_2 to zirconates at moderate temperatures. A great deal has also been learned about ways in which ZrI_4 can be sequestered in reduced zirconium iodide phases, particularly those such as $Zr_6I_{12}C$ that are greatly stabilized by a common impurity such as carbon.[2,11]

The actual detection of cesium zirconates (as well as probable zirconium iodide phases) in used fuel rods has not been accomplished unambiguously. This process is made difficult not only by the intense radiation present but also by the high proclivity of both types of products to hydrolysis. The latter factor has generally not been taken into consideration in postfission examinations of fuel rods.

Acknowledgment. We are particularly indebted to Professor R. Hoppe for his interest in this work and for his provision of both the MAPLE calculations and information on related research that has taken place at Giessen. We also acknowledge the continuing provision of X-ray diffractometer facilities by Professor R. A. Jacobson.

Supplementary Material Available: Tables of anisotropic thermal ellipsoid parameters for the atoms in Cs_2ZrO_3 (1 page); table of observed and calculated structure factors for Cs_2ZrO_3 (1 page). Ordering information is given on any current masthead page.

Preparation of Boron-Containing Ceramic Materials by Pyrolysis of the Decaborane(14)-Derived $[-B_{10}H_{12}{\cdot}Ph_2POPPh_2]_x-$ Polymer

Dietmar Seyferth,*,† William S. Rees, Jr.,† John S. Haggerty,*,‡ and Annamarie Lightfoot‡

Department of Chemistry and Materials Processing Center, Massachusetts Institute of Technology, Cambridge, Massachusetts 02139

Received June 13, 1988

The pyrolysis of the known polymer $[-B_{10}H_{12}{\cdot}Ph_2POPPh_2]_x-$ to give a boron-containing ceramic has been studied. The pyrolysis to 1000 °C gives an amorphous solid in 93% ceramic yield that contains boron, phosphorus, oxygen, and a large excess of carbon. Further studies devoted to this material have served to characterize it with respect to surface area, pore size and distribution, density, grain size, crystalline phases, and elemental composition as a function of temperature up to 2350 °C.

Introduction

Polymer pyrolysis as a route to ceramic materials has received much attention in recent years.[1] This procedure has been applied principally to the preparation of silicon-containing ceramic materials such as silicon carbide, nitride, carbonitride, and oxynitride.[1,2] Much less work has been devoted to the application of polymer pyrolysis to the preparation of boron-containing ceramic materials. The few reports in this area have dealt mostly with boron nitride precursors,[3] and there is only one recent example of the preparation of boron carbide by the preceramic polymer route.[3h]

The development of polymer pyrolysis as a route to ceramics beyond the restricted field of pyrolytic carbon came about as a result of interest in new "high-technology" applications of ceramics with exceptional high-temperature properties such as the carbides, nitrides, and oxides of silicon, boron, aluminum, and the early transition metals. For instance, there is considerable interest in strong ceramic fibers for use in composites, in inert ceramic coatings for materials that are subject to high-temperature oxidation and other forms of corrosion, and in low-loss binders for use in forming ceramic powders into shaped bodies. These applications require a soluble or fusible polymeric precursor that can be spun into fibers and/or that can be used to coat ceramic bodies and powder particles. Also of interest is the preparation of shaped ceramic bodies by pyrolysis of shaped bodies of such "preceramic" polymers.

The issues that are of importance in preceramic polymer design and preparation have been discussed.[1] The most important *chemical* issues are those of polymer processability, high ceramic yield, and elemental composition. However, there are important *ceramics* issues as well, such

† Department of Chemistry.
‡ Materials Processing Center.

(1) Reviews on preceramic polymers: (a) Wynne, K. J.; Rice, R. W. *Ann. Rev. Mater. Sci.* **1984**, *14*, 297. (b) Rice, R. W. *Am. Ceram. Soc. Bull.* **1983**, *62*, 889. (c) Seyferth, D. In *Transformations of Organometallics Into Common and Exotic Materials: Design and Activation*; NATO ASI Series E: Applied Sciences, 141; Laine, R. M., Ed.; Martinus Nijhoff: Dordrecht, 1988; pp 133–154. (d) Seyferth, D.; Wiseman, G. H.; Schwark, J. M.; Yu, Y.-F.; Poutasse, C. A. In *Inorganic and Organometallic Polymers*; ACS Symposium Series 360; Zeldin, M., Wynne, K. J., Allcock, H. R., Eds.; American Chemical Society: Washington, D.C., 1988; pp 143–155.

(2) (a) Yajima, S. *Am. Ceram. Soc. Bull.* **1983**, *62*, 893. (b) Wills, R. R.; Markle, R. A.; Mukherjee, S. P. *Am. Ceram. Soc. Bull.* **1983**, *62*, 904. (c) Schilling, Jr., C. L.; Wesson, J. P.; Williams, T. C. *Am. Ceram. Soc. Bull.* **1983**, *62*, 912. (d) LeGrow, G. E.; Lim, T. F.; Lipowitz, J.; Reaoch, R. S. *Am. Ceram. Soc. Bull.* **1987**, *66*, 363. (e) Laine, R. M.; Blum, Y. D.; Tse, D.; Glaser, R. In *Inorganic and Organometallic Polymers*; ACS Symposium Series 360; Zeldin, M., Wynne, K. J., Allcock, H. R., Eds.; American Chemical Society: Washington, D.C.; 1988; pp 124–142.

(3) (a) Narula, C. K.; Schaeffer, R.; Paine, R. T.; Dayte, A., Hammetter, W. F. *J. Am. Chem. Soc.* **1987**, *109*, 5556. (b) Narula, C. K.; Janik, J. F.; Duesler, E. N.; Paine, R. T.; Schaeffer, R. *Inorg. Chem.* **1986**, *25*, 3346. (c) Wada, H.; Ito, S.; Kuroda, K.; Kato, C. *Chem. Lett.* **1985**, 691. (d) Pacioreck, K. J. L.; Kratzer, R. H.; Harris, D. H.; Smythe, M. E.; Kimble, P. F. U.S. Patent 4581468, 1986. (e) Pacioreck, K. J. L.; Harris, D. H.; Kratzer, R. H. *J. Polym. Sci., Polym. Chem. Ed.* **1986**, *24*, 173. (f) Lindemanis, A. E. *Mater. Sci. Res.* **1984**, *17*, pp 111–121. (g) Rees, Jr., W. S.; Seyferth, D. *J. Am. Ceram. Soc.* **1988**, *71*, C-194. (h) Mirabelli, M. G. L.; Sneddon, L. G. *J. Am. Chem. Soc.* **1988**, *110*, 3305.

0897-4756/89/2801-0045$01.50/0